Available online at www.sciencedirect.com
ScienceDirect
Applied Soft Computing 8 (2008) 1453–1462
Applied Soft Computing
www.elsevier.com/locate/asoc

Differential Evolution as a viable tool for satellite image registration

I. De Falco [a,*], A. Della Cioppa [b], D. Maisto [a,c], E. Tarantino [a]

[a] Institute of High Performance Computing and Networking, National Research Council of Italy (ICAR-CNR), Via P. Castellino 11, 80131 Naples, Italy
[b] Natural Computation Lab – DIIIE, University of Salerno, Via Ponte Don Melillo 1, 84084 Fisciano (SA), Italy
[c] School of Graduate Studies, University of Modena and Reggio, Via Campi, 41100 Modena, Italy

Received 31 January 2007; received in revised form 5 September 2007; accepted 21 October 2007
Available online 4 December 2007

Abstract

A software system grounded on Differential Evolution to automatically register multiview and multitemporal images is designed, implemented and tested through a set of 2D satellite images on two problems, i.e. mosaicking and changes in time. Registration is effected by looking for the best affine transformation in terms of maximization of the mutual information between the first image and the transformation of the second one, and no control points are needed in this approach. This method is compared against five widely available tools, and its effectiveness is shown.

Keywords: Differential Evolution; Image registration; Remote sensing; Affine transformation; Mutual information

1. Introduction

Registration is a fundamental task in image processing. During the years several techniques have been developed for various applications resulting in several methods [1,2]. Typically, the registration is a crucial step in the fields of computer vision [3–19] of medical imaging [20–33] and of remote sensing [34–49].

Image registration methods proposed in literature consist of the following four steplike components [1,2]:

- *Feature detection*. Prominent and distinctive objects (closed-boundary regions, edges, contours, corners, line intersections, etc.) are manually or, preferably, automatically detected. For further processing, these features can be represented by their point representatives (centers of gravity, line endings, distinctive points), called control points.
- *Feature matching*. The correspondence between the features detected in the sensed image and those identified in the reference image is verified. To this aim feature descriptors and similarity measures along with spatial relationships among the features are used.
- *Transform model estimation*. The type and parameters of the so-called mapping functions, aligning the sensed image with the reference image, are estimated. The parameters of the mapping functions are calculated by means of the established feature correspondence. According to the transformation model used, mapping functions can be classified into linear transformations which are a combination of translation, rotation, global scaling, shear and perspective components, and elastic or 'nonrigid' transformations which allow local warping of image features.
- *Image resampling and transformation*. The sensed image is transformed by means of the mapping functions. Image values in non-integer coordinates are computed by the appropriate interpolation technique.

Among the transformation methods, the one based on the use of an affine transformation [50] to ''align'' at best the two images to be registered appears of interest in many fields of application. Then the problem becomes that of finding the best among all the possible transformations, each of which is represented by a set of real parameters. An exhaustive search becomes impracticable in case of diverse degrees of freedom of the transformation, and thus heuristic optimization algorithms are helpful. As Evolutionary Algorithms (EAs) [51–54] are successfully applied to face several multivariable optimization tasks, their use has been introduced in image registration as well, in particular in the medical [55–64] and in the remote sensing [65–73] areas.

The goal of the paper consists in the design and implementation of an evolutionary system for the registration of images by using the affine transformation model.

* Corresponding author.
E-mail address: ivanoe.defalco@na.icar.cnr.it (I. De Falco).

1568-4946/$ – see front matter
doi:10.1016/j.asoc.2007.10.013

Differential Evolution (DE) [53,74] is a version of an EA which has proven fast and reliable in many applications [75–77]. Therefore, we have implemented a DE algorithm to find the optimal combination of the parameter values involved in the affine transformation. There exist in literature several approaches based on either explicitly providing a set of control points [34,70,78–80](including DE [81]) or in automatically extracting them from the image [82,83,43]. In contrast to those approaches, here we wish to examine DE ability to perform automatic image registration without making any use of control points. This evolutionary system will be tested by means of a set of 2D satellite images.

Paper structure is as follows: Section 2 describes the image registration problem and defines the affine transformation and the mutual information. Section 3 contains DE basic scheme and illustrates the application of our system to the registration task. Section 4 reports on the two remote sensing problems faced, i.e. mosaicking and changes in time, and shows the results achieved by our tool and their comparison against those provided by five widely available registration tools. Finally Section 5 contains conclusions and future works.

2. Image registration

Registration is often necessary for integrating information taken from different sensors (*multimodal analysis*), or finding changes in images acquired under diverse viewing angles (*multiview analysis*) or disparate times (*multitemporal analysis*). Depending on the application, the goals of registering images may be quite different. In remote sensing two problems are usually faced, i.e. *Mosaicking* and *Change Discovery*. The former is an example of *multiview analysis* and deals with spatially aligning two images of neighboring areas taken at the same time so as to obtain a larger view of the surveyed scene, whereas the latter, representing a *multitemporal analysis* application, consists in firstly aligning two images of about the same area but acquired at different times, and then in pointing out the changes happened in that area within the difference timespan. In all cases, two choices must be made to carry out image registration. The first choice involves the kind of geometric transformation to be considered to find correlations between the given images, while the second one concerns the measure of match (MOM), i.e. the feature on the value of which the goodness of the registration is evaluated. Once made these choices, the MOM can be maximized by using suitable optimization algorithms.

2.1. Affine transformation

The most frequently used transformation model in registration applications is the affine transformation. This model is sufficiently general, since it can handle rotations, translations, scaling and shearing. This transformation can be represented in the most general 3D case as

$$\mathbf{x}' = A \cdot \mathbf{x} + \mathbf{b} \tag{1}$$

where A is a 3×3 square matrix accounting for rotations and scalings while $\mathbf{x}, \mathbf{x}'$ and $\mathbf{b}$ are three-dimensional arrays representing respectively the original positions, the transformed ones and a translation vector.

2.2. Mutual information

The most widely employed MOM is the mutual information (MI) [84,85], which represents the relative entropy of the two images to be aligned. The greater the value of MI, the better the match between the two images, so this becomes a typical maximization problem.

In general, given two random variables Y and Z, their MI is

$$I(Y,Z) = \sum_{y,z} P_{Y,Z}(y,z) \log \frac{P_{Y,Z}(y,z)}{P_Y(y) \cdot P_Z(z)} \tag{2}$$

where $P_Y(y)$ and $P_Z(z)$ are the marginal probability mass functions and $P_{Y,Z}(y,z)$ is the joint probability mass function. MI is related to entropies by

$$I(Y,Z) = H(Y) + H(Z) - H(Y,Z) \tag{3}$$

with $H(Y,Z)$ being their joint entropy, and $H(Y)$, $H(Z)$ the entropies of Y and Z, respectively. The definitions of these entropies are

$$\begin{aligned} H(Y) &= -\sum_{y} P_Y(y) \log P_Y(y), \\ H(Z) &= -\sum_{z} P_Z(z) \log P_Z(z) \end{aligned} \tag{4}$$

$$H(Y,Z) = -\sum_{y,z} P_{Y,Z}(y,z) \log P_{Y,Z}(y,z) \tag{5}$$

To employ MI as a similarity measure, the 2D histogram of an image pair, the joint histogram h, must be utilized. It is defined as a function of two variables Y and Z, the gray-level intensities in the two images. Its value at the coordinate (Y,Z) is the number of corresponding pairs having gray-level Y in the first image and gray-level Z in the second image. The joint probability mass function of an image pair is then obtained by normalizing the joint histogram of the image pair:

$$P_{Y,Z}(y,z) = \frac{h(y,z)}{\sum_{y,z} h(y,z)} \tag{6}$$

From it the two marginal probability mass functions can be obtained as

$$P_Y(y) = \sum_{z} P_{Y,Z}(y,z), \qquad P_Z(z) = \sum_{y} P_{Y,Z}(y,z) \tag{7}$$

The MI registration criterion states that the image pair is geometrically aligned through a geometric transformation $\mathbf{T}$ when $I(Y(\mathbf{x}), Z(\mathbf{T}(\mathbf{x})))$ is maximal. Thus, the aim is to maximize Eq. (3).

The MI methods represent the leading technique in image registration. Depending on the degrees of freedom of the geometric transformation, the search of an optimal similarity measure results in a more or less difficult task, especially if one

considers that small parameter changes may determine meaningful variations in this measure. Several techniques have been proposed to face this problem [86,87,84,88,89]. Here a Differential Evolution algorithm is taken into account.

3. Differential Evolution

Differential Evolution (DE) is a stochastic, population-based optimization algorithm [53,74]. It was firstly developed to optimize real parameters of a real-valued function and uses vectors of real numbers as representations of solutions. The seminal idea of DE is that of using vector differences for perturbing the genotype of the individuals in the population. Basically, DE generates new individuals by adding the weighted difference vector between two population members to a third member. This can be seen as a non-uniform crossover that can take child vector parameters from one parent more often than it does from others. If the resulting trial vector yields a better objective function value than a predetermined population member, the newly generated vector replaces the vector with which it was compared. By using components of existing population members to construct trial vectors, recombination efficiently shuffles information about successful combinations, enabling the search for an optimum to focus on the most promising area of solution space. In more detail, given a maximization problem with m real parameters, DE faces it starting with a randomly initialized population consisting of n individuals each made up by m real values. Then, the population is updated from a generation to the next one by means of many different transformation schemes. In all of these schemes DE basicly generates new individuals by adding to a member a number of weighted difference vectors between couples of population members. We have decided to perturb a random individual by using one difference vector and by applying binomial crossover, so our strategy can be referenced as *DE/rand/1/bin*. In it for the generic ith individual in the current population three integer numbers r_1, r_2 and r_3 in $[1, n]$ differing one another and different from i are randomly generated. Furthermore, another integer number k in the range $[1, m]$ is randomly chosen. Then, starting from the ith individual a new trial one i' is generated whose generic jth component is given by

$$x_{i',j} = x_{r_3,j} + F \cdot (x_{r_1,j} - x_{r_2,j}) \tag{8}$$

provided that either a random real number ρ in $[0.0, 1.0]$ is lower than a value CR (parameter of the algorithm, in the same range as ρ) or the position j under account is exactly k. If neither is verified then a copy takes place: $x_{i',j} = x_{i,j}$. F is a real and constant factor in $[0.0, 1.0]$ which controls the magnitude of the differential variation $(x_{r_1,j} - x_{r_2,j})$, and is a parameter of the algorithm.

This new trial individual i' is compared against the ith individual in current population and, if fitter, replaces it in the next population, otherwise the old one survives and is copied into the new population. This basic scheme is repeated for a maximum number of generations g.

By using components of existing population members to construct trial vectors, recombination efficiently shuffles information about successful combinations, enabling the search for an optimum to focus on the most promising area of solution space.

3.1. DE for Image Registration

3.1.1. Encoding

We have decided to make use of the aforementioned affine transformation model. Since the experiments reported in this paper make reference to couples of two-dimensional images, Eq. (1) reduces to

$$x'_1 = a_{11}x_1 + a_{12}x_2 + b_1, \qquad x'_2 = a_{21}x_1 + a_{22}x_2 + b_2 \tag{9}$$

so the whole problem consists in finding the best combination of six real-valued parameters. Therefore, any individual in the DE population is an array with six positions, with the parameters listed as follows: $\mathbf{T} = (a_{11}, a_{12}, a_{21}, a_{22}, b_1, b_2)$ and each parameter can vary within a range of its own.

3.1.2. Fitness

Given two images C and D we take as fitness function their mutual information I, so the aim of the problem becomes to find the best affine transformation $\mathbf{T}$ for D such that the mutual information of C and $\mathbf{T}(D)$ is maximized.

4. Experiments and findings

We have faced both *Mosaicking* and *Change Discovery* problems typical of remotely sensed image registration, as examples of multiview and multitemporal analysis, respectively. The first, named below as *Mosaic*, accounts for the registration of two images of the same scene acquired from different viewpoints while the second, referred to as *Changes*, looks for the changes in an area by examining two images taken at different times.

In both cases DE parameters have been set as follows: $n = 30$, $g = 200$, CR = 0.5 and $F = 0.5$. No preliminary tuning phase has been performed. It is important to remark here that, differently from some papers in literature about use of EAs to solve this task, as for example [26,90,91], we have decided to use quite wide ranges for each variable in the $\mathbf{T}$ solution, since we hope that evolution drive the search towards good transformations. The allowed variation ranges are shown in Table 1.

For each problem 20 DE runs have been carried out, so as to investigate the dependence of the results on the initial random

Table 1
Problem variable ranges

	a_{11}	a_{12}	a_{21}	a_{22}	b_1	b_2
Min.	0.500	−0.500	−0.500	0.500	−200.0	−200.0
Max.	1.500	0.500	0.500	1.500	200.0	200.0

seed. The best of those runs will be discussed below in terms of image transformation achieved and of evolution.

4.1. The Mosaic task

In the first test case we have used two images which are portions of a Landsat Thematic Mapper (TM) digital image recorded on 7 September 1984 over San Francisco bay area (CA, USA) (property of United States Geological Survey [92]). Those images were transformed by us into grey monochannel images, so that each of them is 500×500 pixel large and uses 8 bits to represent each pixel. Fig. 1 shows them both. Their I value is 0.1732. Fig. 2 (top left) reports the fusion of the two original images. They share a common area, which should be used by the DE algorithm to find their best registration. Namely, the up-left part of the second image overlaps the bottom-right part of the first, and a slight clockwise rotation was applied to the second image with reference to the first one. So, the best affine transformation should contain a slight counterclockwise rotation and two positive shifts for both the coordinates.

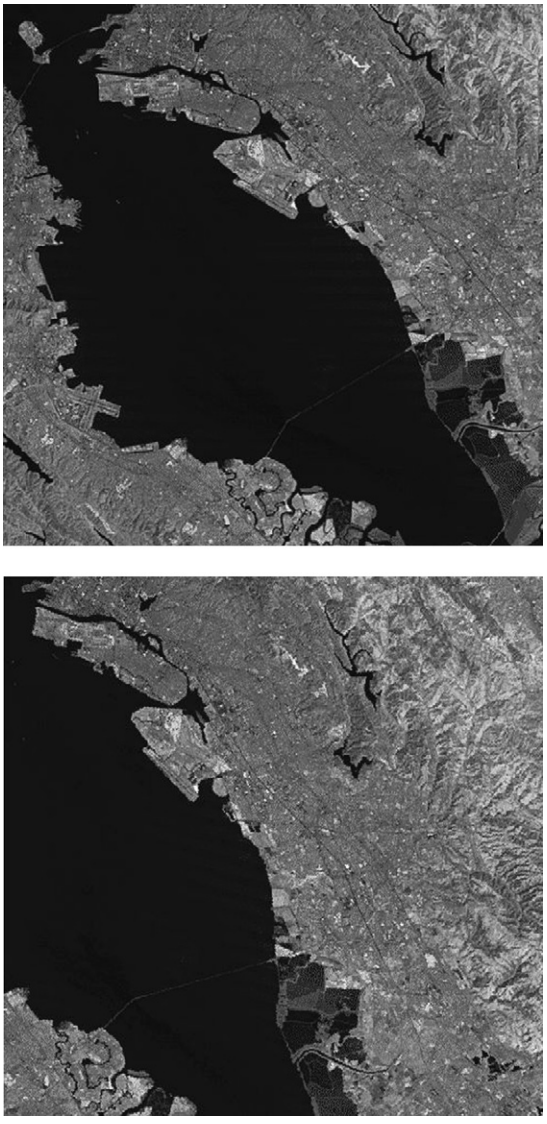

Fig. 1. The two original *Mosaic* images.

In this problem the best value of I obtained in the best execution is 1.1083. The average of the best final values over the 20 runs is 0.9068 and the variance is 0.1378, the worst result being 0.6351. The best affine transformation found is

$$\begin{aligned} x_1' &= 0.946x_1 - 0.253x_2 + 41.858, \\ x_2' &= 0.253x_1 + 0.946x_2 + 49.779 \end{aligned} \tag{10}$$

which represents a counterclockwise rotation of about 15° coupled with a translation in both axes. The resulting transformed image is shown in Fig. 2 (top right). Fig. 2 (bottom left) depicts the fusion of the first original image with the best transformation found for the second one. The alignment of the two registered images is excellent: any detail in the first image, from the streets to the shoreline to the bridges, is perfectly aligned with the corresponding pixels representing it in the transformed second image. In Fig. 2 (bottom right), we report the behavior of the best run achieved for the *Mosaic* task. In this case, in spite of the very relaxed parameter range allowed, already the initial population achieves an improving solution with respect to the original one. From then on the system proposes many improving affine transformations and both the average and the best fitness values increase over generations until the end of the run.

4.2. The Changes task

In the second test case we have used two images which refer to about the same area but were taken at different times. Namely, they represent an agricultural area near San Francisco (CA, USA) in 1984 and in 1993 respectively (they too are property of USGS [92]). As before, the original Landsat TM images were transformed by us into grey monochannel images, so that each of them is 500×500 pixel large with an 8-bit representation for each pixel (see Fig. 3). Their I value is 0.1123. Fig. 4 (top left) reports the fusion of the two original images. As it can be observed, they share a common area, which should be used by the DE algorithm to find their best registration. Namely, the right part of the first image overlaps the left part of the second, and a slight clockwise rotation took place when the second image was taken with reference to the first one. So, the best affine transformation should contain a slight counterclockwise rotation and some shifts for both the coordinates.

In this problem the best value of I attained in the best execution is 0.3951. The average of the best final values over the 20 runs is 0.3918 and the variance is 0.0049, the worst result being 0.3803. The best affine transformation found is

$$\begin{aligned} x_1' &= 0.954x_1 - 0.083x_2 + 16.995, \\ x_2' &= 0.083x_1 + 0.953x_2 + 20.361 \end{aligned} \tag{11}$$

which represents a counterclockwise rotation of about 5° coupled with a translation in both axes. The resulting transformed image is shown in Fig. 4 (top right). Fig. 4 (bottom left)

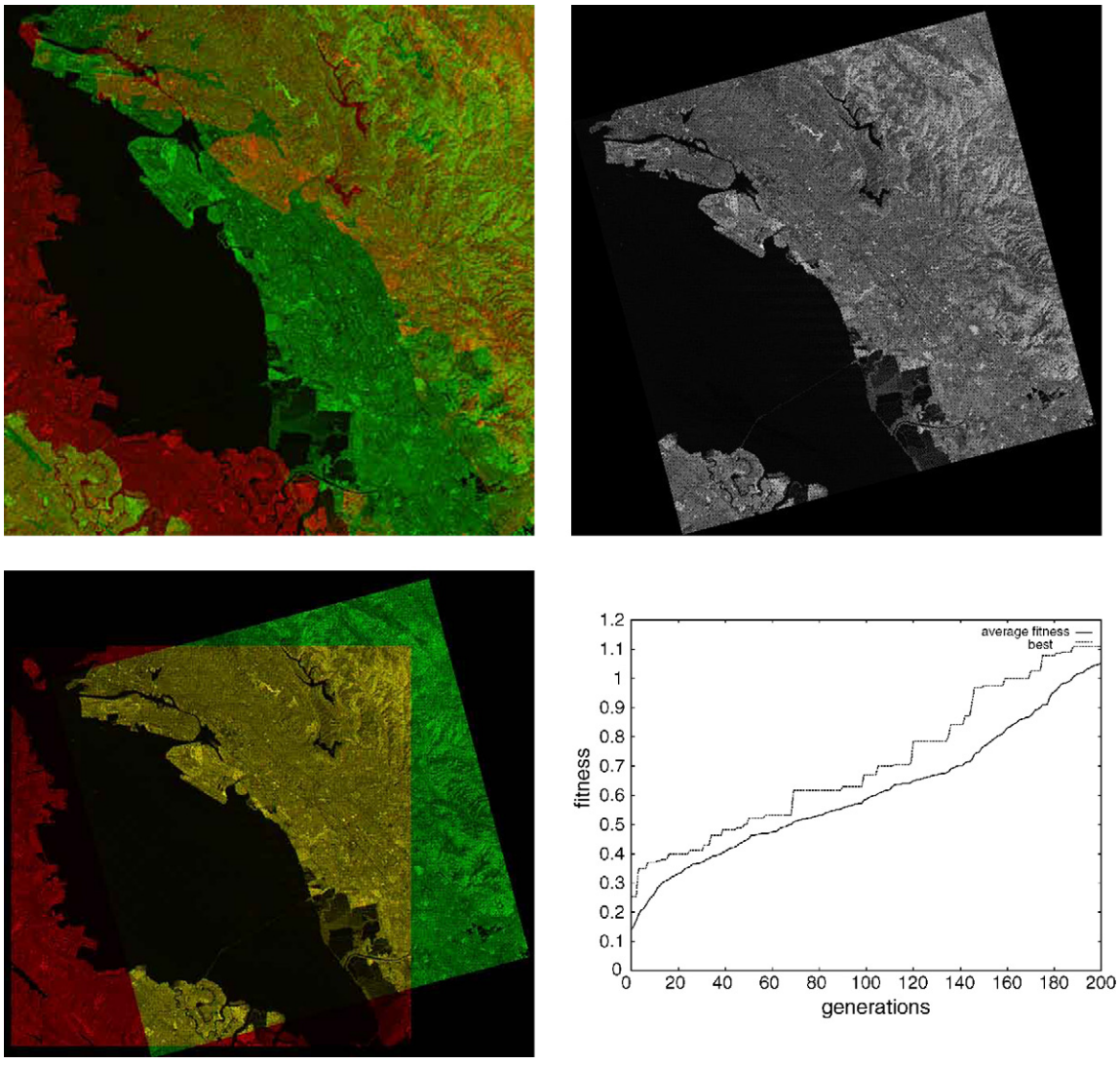

Fig. 2. Top left: the fusion of the two original images. Top right: the best transformation for the second *Mosaic* image. Bottom left: the first image is fused with the best transformation found for the second one. Bottom right: behavior of fitness as a function of the number of generations for the best run.

shows the fusion of the first original image with the best transformation found for the second one. The alignment of the two registered images is very good: any detail in the first image, from the rivers to the roads to the fields, is well aligned with the corresponding pixels representing it in the transformed second image. Fig. 4 (bottom right) presents the behavior of the best run achieved for the *Changes* task. Also in this case, in spite of the very relaxed parameter range allowed, already the initial population achieves an improving solution with respect to the original one and from then on the system proposes many improving affine transformations and both the average and the best fitness values increase over generations until the end of the run.

The computed differences between the first image and the transformed second one are shown in Fig. 5, where only the part in which the two images overlap is meaningful. In it the grey color refers to areas where no changes occurred, the black represents areas that were burned in 1984 and recovered by 1993, whereas the white stands for areas more vegetated in 1984 than in 1993 due to differences in the amount of rainfall, or to the density or level of maturity of the vegetation. Light pixels represent areas burned in 1993 or which were natural landscape areas in 1984 that were converted to agricultural lands and recently tilled, and finally dark pixels stand for areas more vegetated in 1993 than in 1984.

4.3. Comparison and discussion

To investigate the goodness of the results achieved by our tool on the two tasks, we have compared them against those provided by a set of widely available image registration tools. Firstly, we have taken into account *ImReg* [93], developed at the Vision Research lab at the University of Santa Barbara, USA [94]. A user needs to upload the two images to its internet site and to set a parameter about the desired registration quality (fast, normal, quality, extra). *ImReg* is based on the following steps: automatical retrieval of a set of tie points, search of the transformation using geometry of tie points, cull of bad tie

Fig. 3. The two original *Changes* images.

points which do not match this transformation, and finally test of the achieved transformation. We have always used extra quality mode. Since this method has no parameters, only one run can be carried out on any couple of images.

Then we have considered the Image Registration tool (*IRT*) contained in the Image Processing toolbox of Matlab 7 [95]. The toolbox provides an interactive tool, called the Control Point Selection Tool, that is used by the user to manually pick pairs of corresponding control points in both images. Control points are landmarks that can be found in both images, like a road intersection, or a natural feature. Of course, different sets of control points will determine different transformations. Then, once chosen the kind of transformation (linear conformal, affine, projective, polynomial) *IRT* will correct the type of distortion present in the base image, determining the parameters of the spatial transformation and transforming the input image to bring it into alignment with the base image. In this case we have chosen an affine transformation and we have performed 20 different runs (corresponding to 20 different choices for the control points) for any pair of images.

Thirdly, we have run a contour-based registration tool again developed at the University of Santa Barbara, USA, and freely downloadable, i.e. *Xreg* [96]. Its contour matching algorithm is based on the chain-code correlation and other shape similarity criteria such as invariant moments. This approach extracts contour information from each of two images and correlates salient features of the contours: closed contours and the salient segments along the open contours are matched separately. Then *Xreg* finds optimal transform parameters for aligning the images and registers them. Finally the images are combined to present the result. This method is claimed to work well for image pairs in which the contour information is well preserved, such as the optical images from Landsat and Spot satellites. This algorithm does not depend on external parameters, so only one run has been carried out.

Furthermore, we have used another freely downloadable software tool, *RegiStar* [97], which is an image alignment, or registration, program that was designed to work specifically with astronomical images. *RegiStar* finds the stars or other control points in an image, and uses their positions to align this image to another image or group of images. *RegiStar* uses a sophisticated matching algorithm that allows images at different scales and orientations to be registered and automatically corrects for geometric distortions. It has no parameters, so only one run can be effected.

Finally, we have also tested the capabilities of *TurboReg* [98], which can be freely downloaded from the site of the Biomedical Imaging Group at the Ecole Polytechnique Federale de Lausanne [99]. It is provided as a plugin for the *Image processing and Analysis in Java* (ImageJ) tool [100], a public domain Java image processing program developed at the National Institute for Mental Health, USA. *TurboReg* is an automatic sub-pixel registration algorithm that minimizes the mean square difference of intensities between a pair of 2D or 3D images, uses spline processing, is based on a coarse-to-fine strategy (pyramid approach), and performs minimization according to a new variation of the iterative Marquardt-Levenberg algorithm for non-linear least-square optimization (MLA). The geometric deformation model is an affine transformation. This method is claimed to achieve excellent results in the medical domain. Since this tool is automatic, only one run has been performed.

The results achieved on the *Mosaic* task are summarized in Table 2. In it we report for any technique the value of the mutual information for the best solution found I_b, and, when meaningful, the average value over the runs $\langle I \rangle$, the related variance σ_I and the worst among the best final values found for the mutual information over the 20 runs I_w. Furthermore, for any technique the best solution found is shown. As it can be seen, our DE-based tool achieves the best performance in terms of higher mutual information, and all other methods find solutions with values of I much lower than that found by DE tool, even in its worst case. Then, *TurboReg* is in this case the second tool in terms of solution quality.

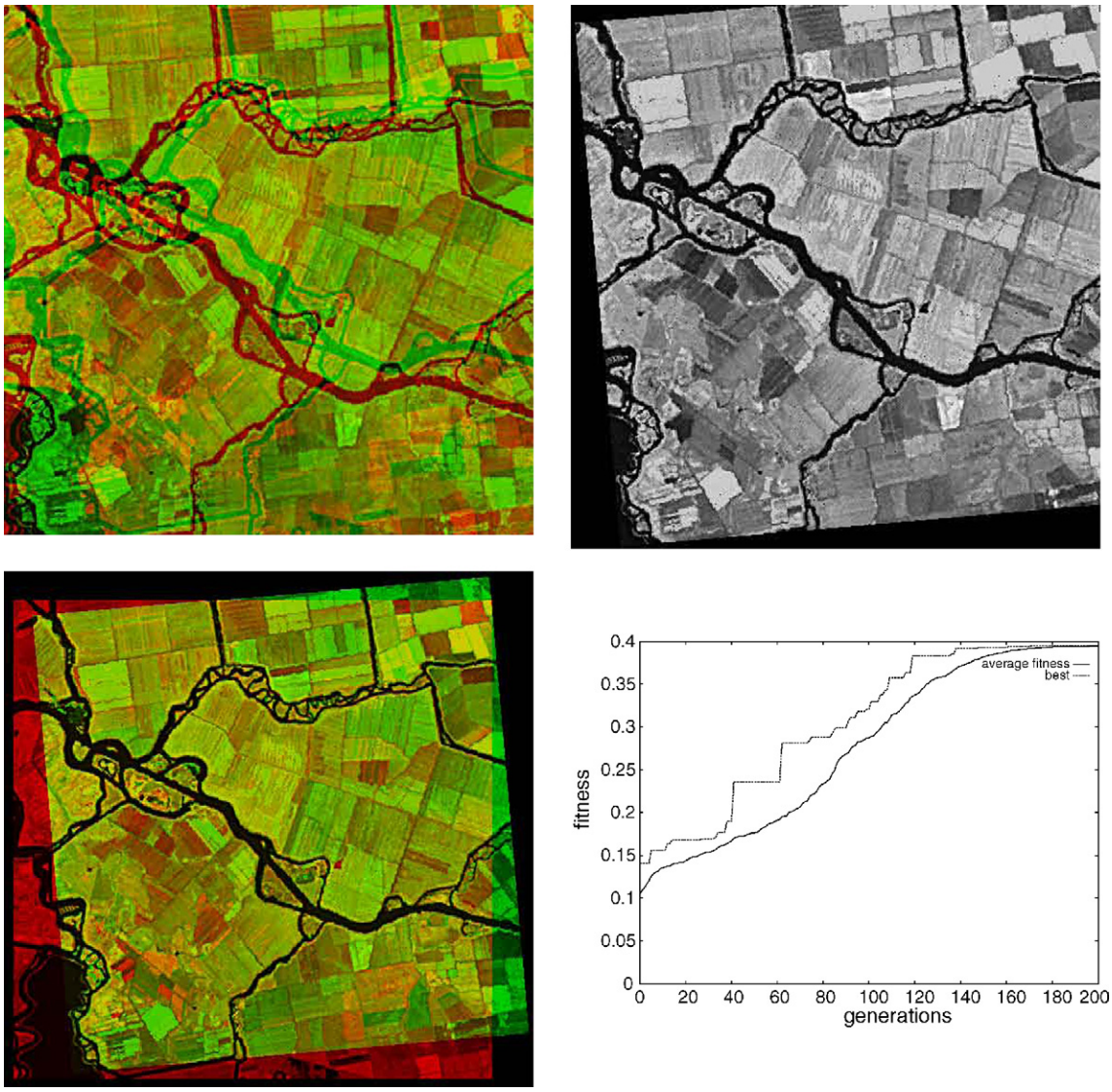

Fig. 4. Top left: the fusion of the two original images. Top right: the best transformation for the second *Changes* image. Bottom left: the first image is fused with the best transformation found for the second one. Bottom right: behavior of fitness as a function of the number of generations for the best run.

Similarly, Table 3 contains the results for the *Changes* task. Also in this case DE turns out to be the best technique, though in this case its superiority with respect to *IRT* is less impressive. The other methods, instead, keep on being very far from ours and for this problem too the solutions provided by the other methods are much lower than those found by our tool, even in its worst case. It should be remarked here that *Registar* is not able to carry out the registration task on this couple of images. Moreover it is worth noting that *TurboReg* shows quite poor performance in this case, although it works well on the *Mosaic* task. These two latter considerations lead us to suppose that the *Changes* task is more difficult than expected.

It should be noted that the values of the parameters reported in Tables 2 and 3 are truncated at the third decimal digit. In fact, in some cases, the difference between the value of the same parameter provided by different methods is in the order of 10^{-5} to 10^{-6}. Furthermore, the experimental analysis has proved that small variations in the parameter values may result in

Table 2
Results on *Mosaic* task

Method	I_b	$\langle I \rangle$	σ_I	I_w	a_{11}	a_{12}	a_{21}	a_{22}	b_1	b_2
DE	1.1083	0.9068	0.1378	0.6351	0.946	−0.253	0.253	0.946	41.858	49.779
ImReg	0.3984	–	–	–	0.984	−0.263	0.263	0.984	53.687	37.667
IRT	0.4719	0.4377	0.365	0.0379	0.944	−0.256	0.256	0.947	49.180	42.365
Xreg	0.4748	–	–	–	0.966	−0.259	0.259	0.966	36.690	53.647
RegiStar	0.5342	–	–	–	0.967	−0.256	0.256	0.967	33.051	46.127
TurboReg	0.5704	–	–	–	0.966	−0.259	0.259	0.966	38.384	45.065

Table 3
Results on *Changes* task

Method	I_b	$\langle I \rangle$	σ_I	I_w	a_{11}	a_{12}	a_{21}	a_{22}	b_1	b_2
DE	0.3951	0.3918	0.0049	0.3803	0.954	−0.083	0.083	0.953	16.995	20.361
ImReg	0.1456	–	–	–	1.041	−0.088	0.088	1.041	18.845	19.437
IRT	0.3188	0.2090	0.0767	0.144	0.952	−0.083	0.085	0.950	17.997	18.907
Xreg	0.1816	–	–	–	0.997	−0.070	0.070	0.997	17.332	22.094
RegiStar	–	–	–	–	–	–	–	–	–	–
TurboReg	0.1325	–	–	–	0.979	−0.202	0.202	0.979	−40.795	50.406

Fig. 5. *Changes* image in an agricultural area near San Francisco within 1984 and 1993.

meaningful changes in the value of I, thus evidencing that we are dealing with a rugged fitness landscape.

Another important remark which can be drawn by looking at Tables 2 and 3 is that in both problems the variance shown by *DE* is much lower than that of the other registration tool based on multiple runs, i.e. *IRT*. This is a very important feature of our algorithm, since implies that it is less dependent on the initial configuration (in this case, the seed for the random number generator) than *IRT*. Actually, the performance of this latter strongly depends on the choice of the positions of the user-defined control points: the farther one another, the more accurate the resulting registration.

As a conclusion, we have that for both problems our system achieves better solutions than all other methods in terms of higher mutual information, which proves the quality of our approach.

5. Conclusions and future works

In this paper a Differential Evolution strategy has been coupled with affine transformation and Mutual Information maximization to perform automatic registration of remotely sensed images without considering any kind of control points. A comparison has been carried out against five widely available registration tools on two classical problems. The results show that our evolutionary system outperforms the others, and seem to imply that this approach is promising, yet there is plenty of work still to do. Therefore, future works shall aim to evaluate the effectiveness of our system in this field, and its limitations as well.

Firstly, a wide tuning phase shall be carried out to investigate if some DE parameter settings are, on average, more useful than others. Moreover, we aim to apply our approach also to multimodal analysis in remote sensing, as for example fusion of information from sensors of different characteristics. Furthermore we plan to implement a coarse-grained parallel version of the DE algorithm based on the island model, and to run it on a cluster of workstations.

Lastly, our final goal is to design and implement a technique which could be useful also for 3D multimodal medical image registration.

References

[1] L.G. Brown, A survey of image registration, ACM Comput. Surveys 24 (4) (1992) 325–376.
[2] B. Zitova, J. Flusser, Image registration methods: a survey, Image Vision Comput. 21 (2003) 977–1000.
[3] Q. Zheng, R. Chellappa, A computational vision approach to image registration, IEEE Trans. Image Process. 2 (3) (1993) 311–326.
[4] G. Blais, M.D. Levine, Registering multiview range data to create 3d computer objects, IEEE Trans. Pattern Anal. Mach. Intell. 17 (1995) 820–824.
[5] C. Dorai, G. Wang, A.K.J.C. Mercer, Registration and integration of multiple object views for 3d model construction, IEEE Trans. Pattern Anal. Mach. Intell. 20 (1) (1998) 83–89.
[6] J.P. Tarel, N. Boujemaa, A coarse to fine 3d registration method based on robust fuzzy clustering, Comput. Vision Image Understanding 73 (1) (1999) 14–28.
[7] A. Giachetti, Matching techniques to compute image motion, Image Vision Comput. 18 (2000) 247–260.
[8] J. Williams, M. Bennamoun, Simultaneous registration of multiple corresponding point sets, Comput. Vision Image Understanding 73 (2001) 117–142.
[9] Y. Caspi, M. Irani, Aligning non-overlapping sequences, Int. J. Comput. Vision 48 (1) (2002) 39–51.
[10] T. Masuda, Registration and integration of multiple range images by matching signed distance fields for object shape modeling, Comput. Vision Image Understanding 87 (2002) 51–65.
[11] K. Rohr, M. Forenefett, H.S. Stiehl, Spline-based elastic image registration: Integration of landmark errors and orientation attributes, Comput. Vision Image Understanding 90 (2003) 153–168.
[12] X. Yu, H. Sun, Automatic image registration via clustering and convex hull vertices matching, Lecture Notes in Computer Science – Advanced Data Mining Applications, vol. 3584, Springer-Verlag, 2005, pp. 439–445.
[13] J. Reisman, U. Uludag, A. Ross, Secure fingerprint matching with external registration, in: Proceedings of the Fifth International Conference on Audio and Video-Based Biometric Person Authentication, Hilton Rye Town, NY, USA, (2005), p. 720.

[14] X. Huang, N. Paragios, D. Metaxas, Shape registration in implicit spaces using information theory and free form deformations, IEEE Trans. Pattern Anal. Mach. Intell. 28 (8) (2006) 1303–1318.
[15] A. Salah, L. Akarun, 3d facial feature localization for registration, in: Lecture Notes in Computer Science, vol. 4105, Springer-Verlag, 2006, pp. 338–345.
[16] A. Zouhar, T. Fang, G. Unal, G. Slabaugh, H. Xie, F. McBagonluri, in: Proceedings of the Third International Symposium on 3d Data Processing Visualization and Transmission, University of North Carolina, Chapel Hill, USA, (2006), pp. 240–247.
[17] A. Salah, H. Cinar, L. Akarun, B. Sankur, Robust facial landmarking for registration, Ann. Telecommun. 62 (1/2) (2007) 1608–1633.
[18] N. Salah, A.A. Alyuz, L. Akarun, Alternative face models for 3d face registration, in: Proceedings of SPIE, vol. 6499, SPIE, 2007.
[19] L. Liu, T. Jiang, J. Yang, C. Zhu, Fingerprint registration by maximization of mutual information, IEEE Trans. Image Process. 15 (5) (2006) 1100–1110.
[20] G.E. Christensen, R.D. Rabbitt, M.I. Miller, Deformable templates using large deformation kinematics, IEEE Trans. Image Process. 5 (10) (1996) 1435–1447.
[21] J.B.A. Maintz, M.A. Viergever, A survey of medical image registration methods, Med. Image Anal. 2 (1) (1998) 1–37.
[22] H. Lester, S. Arridge, A survey of hierarchical non-linear medical image registration, Pattern Recognit. 32 (1) (1999) 129–149.
[23] P. Hellier, C. Barillot, E. Mémin, P. Pérez, Medical image registration with robust multigrid techniques, in: Lecture Notes in Computer Science, vol. 1679, Springer-Verlag, 1999, pp. 680–687.
[24] D.L.G. Hill, P.G. Batchelor, M. Holden, D.J. Hawkes, Image registration methods: a survey, Phys. Med. Biol. (2001) 1–45.
[25] T. Makela, P. Clarysse, O. Sipila, N. Pauna, T. Quoc Cuong Pham Katila, I.E. Magnin, A review of cardiac image registration methods, IEEE Trans. Med. Imaging 21 (9) (2002) 1011–1021.
[26] G.C. Sakellaropoulos, G.C. Kagadis, C. Karystianos, D. Karnabatidis, C. Constatoyannis, G.C. Nikoforidis, An experimental environment for the production, exchange and discussion of fused radiology images, for the management of patients with residual brain tumour disease, Med. Inform. Internet Med. 28 (2) (2003) 135–146.
[27] C. Guetter, C. Xu, F. Sauer, J. Hornegger, Learning based non-rigid multi-modal image registration using kullback-leibler divergence, in: Proceedings of the Eighth International Conference on Medical Image Computing and Computer-Assisted Intervention, Palm Springs, CA, USA, (2005), pp. 255–262.
[28] L. Wang, M. Greenspan, R. Ellis, Validation of bone segmentation and improved 3-d registration using contour coherency in ct data, IEEE Trans. Med. Imaging 25 (3) (2006) 324–334.
[29] D. Barratt, G. Penney, C. Chan, M. Slomczykowski, T. Carter, P. Edwards, D. Hawkes, Self-calibrating 3d-ultrasound-based bone registration for minimally invasive orthopedic surgery, IEEE Trans. Med. Imaging 25 (3) (2006) 312–323.
[30] F. Richard, P. Bakic, A. Maidment, Mammogram registration: a phantom-based evaluation of compressed breast thickness variation effects, IEEE Trans. Med. Imaging 25 (2) (2006) 188–197.
[31] G. Wu, F. Qi, D. Shen, Learning-based deformable registration of mr brain images, IEEE Trans. Med. Imaging 25 (9) (2006) 1145–1157.
[32] J. Wang, T. Jiang, Nonrigid registration of brain mri using nurbs, Parallel Recognit. Lett. 28 (2) (2007) 214–223.
[33] D. Schwarz, T. Kasparek, I. Provaznik, J. Jarkovsky, A deformable registration method for automated morphometry of mri brain images in neuropsychiatric research, IEEE Trans. Med. Imaging 26 (4) (2007) 452–461.
[34] J. Ton, A.K. Jain, Registering landsat images by point matching, IEEE Trans. Geosci. Remote Sens. 27 (5) (1989) 642–651.
[35] L.M.G. Fonseca, B.S. Manjunath, Registration techniques for multisensor remotely sensed imagery, Photogrammetric Eng. Remote Sens. 62 (9) (1996) 1049–1056.
[36] J. LeMoigne, Towards an intercomparison of automated registration algorithms for multiple source remote sensing data, in: Image Registration Workshop, NASA GSFC, MD, USA, (1997), pp. 307–316.
[37] J. LeMoigne, First evaluation of automatic image registration methods, in: International Geoscience and Remote Sensing Symposium, Seattle, Washington, USA, (1998), pp. 315–317.
[38] C. Lee, J. Bethel, Georegistration of airborne hyperspectral image data, IEEE Trans. Geosci. Remote Sens. 39 (7) (2001) 1347–1351.
[39] J. LeMoigne, W.J. Campbell, R.F. Cromp, An automated parallel image registration technique based on the correlation of wavelet features, IEEE Trans. Geosci. Remote Sens. 40 (8) (2002) 1849–1864.
[40] H. Mahdi, A.A. Farag, Image registration in multispectral data sets, in: International Conference on Image Processing, vol. 2, Rochester, NY, USA, (2002), pp. 369–372.
[41] A. Cole-Rhodes, K. Johnson, J. LeMoigne, I. Zavorin, Multiresolution registration of remote sensing imagery by optimization of mutual information using a stochastic gradient, IEEE Trans. Image Process. 12 (12) (2003) 1495–1511.
[42] H. Chen, P.K. Varshney, M.K. Arora, Mutual information based image registration for remote sensing data, Int. J. Remote Sens. 24 (18) (2003) 3701–3706.
[43] Y. Bentoutou, N. Taleb, K. Kpalma, J. Ronsin, An automatic image registration for applications in remote sensing, IEEE Trans. Geosci. Remote Sens. 43 (9) (2005) 2127–2137.
[44] D. Holland, D. Boyd, P. Marshall, Updating topographic mapping in great Britain using imagery from high-resolution satellite sensors, ISPRS J. Photogrammet. Remote Sens. 60 (3) (2006) 212–223.
[45] E. Lambin, M. Linderman, Time series of remote sensing data for land change science, IEEE Trans. Geosci. Remote Sens. 44 (7) (2006) 1926–1928.
[46] V. Lacroix, M. Idrissa, A. Hincq, H. Bruynseels, O. Swartenbroekx, Detecting urbanization changes using spot5, Parallel Recognit. Lett. 27 (4) (2006) 226–233.
[47] A. Boucher, K. Seto, A. Journel, A novel method for mapping land cover changes: incorporating time and space with geostatistics, IEEE Trans. Geosci. Remote Sens. 44 (11) (2006) 3427–3435.
[48] M. Molinier, J. Laaksonen, T. Hame, Detecting man-made structures and changes in satellite imagery with a content-based information retrieval system built on self-organizing maps, IEEE Trans. Geosci. Remote Sens. 45 (4) (2007) 861–874.
[49] S. Voigt, T. Kemper, T. Riedlinger, R. Kiefl, K. Scholte, H. Mehl, Satellite image analysis for disaster and crisis-management support, IEEE Trans. Geosci. Remote Sens. 45 (6) (2007) 1520–1528.
[50] G.W. Hart, S. Levy, R. McLenaghan, Geometry, in: D. Zwillinger (Ed.), CRC Standard Mathematical Tables and Formulae, CRC Press, Boca Raton, FL, USA, 1995.
[51] D. Goldberg, Genetic Algorithms in Optimization, Search and Machine Learning, Addison Wesley, New York, 1989.
[52] A.E. Eiben, J.E. Smith, Introduction to Evolutionary Computing, Springer, 2003.
[53] K. Price, R. Storn, Differential Evolution, Dr. Dobb's J. 22 (4) (1997) 18–24.
[54] R. Eberhart, Y. Shi, Computational Intelligence: Concepts to Implementations, Morgan Kaufmann, 2003.
[55] J. Jacq, C. Roux, Registration of non-segmented images using a genetic algorithm, Lecture Notes in Computer Science, vol. 905, Springer-Verlag, 1995, pp. 205–211.
[56] C.K. Chow, H.T. Tsui, T. Lee, T.K. Lau, Medical image registration and model construction using genetic algorithms, in: International Workshop on Medical Imaging and Augmented Reality (MIAR '01), IEEE Computer Society, 2001, 174–179.
[57] R. Dony, X. Xu, Differential evolution with powell's direction set method in medical image registration, in: IEEE International Symposium on Biomedical Imaging: From Nano to Macro, IEEE Computer Society, Arlington, VA, USA, (2004), pp. 732–735.
[58] A. Draa, M. Batouche, H. Talbi, A quantum-inspired differential evolution algorithm for rigid image registration, in: Lecture Notes in Computer Science, vol. 3211, Springer, Berlin, Heidelberg, 2004, pp. 147–154.
[59] H. Talbi, M.C. Batouche, Particle swarm optimization for image registration, in: IEEE International Conference on Information and Communication Technologies: From Theory to Applications, vol. 3, IEEE Computer Society, 2004, 397–398.

[60] M. Salomon, G.R. Perrin, F. Heitz, J.P. Armspach, Parallel differential evolution: Application to 3d medical image registration, in: Differential Evolution: A Practical Approach to Global Optimization, Natural Computing Series, Springer-Verlag, 2005, pp. 393–411.
[61] B. Telenczuk, M.J. Ledesma-Carbayo, J.A. Velazquez-Muriel, C.O.S. Sorzano, J.M. Carazo, A. Santos, Molecular image registration using mutual information and differential evolution optimization, in: IEEE International Symposium on Biomedical Imaging: From Nano to Macro, IEEE Computer Society, Arlington, VA, USA, 2006.
[62] O. Cordón, S. Damas, J. Santamaría, Feature-based image registration by means of the chc evolutionary algorithm, Image Vision Comput. 24 (5) (2006) 525–533.
[63] O. Cordón, S. Damas, J. Santamaría, A fast and accurate approach for 3d image registration using the scatter search evolutionary algorithm, Parallel Recognit. Lett. 27 (11) (2006) 1191–1200.
[64] J. Santamaría, O. Cordón, S. Damas, I. Aleman, M. Botella, A scatter search-based technique for pair-wise 3d range image registration in forensic anthropology, in: Soft Computing - A Fusion of Foundations, Methodologies and Applications, vol. 11, Springer-Verlag, (2007), pp. 819–828.
[65] J. Fitzpatrick, J. Grefenstette, D. Gucht, Image registration by genetic search, in: IEEE SoutheastCon Conference, IEEE Computer Society, 1984, 460–464.
[66] D. Dasgupta, D.R. McGregor, Digital image registration using structured genetic algorithms, in: SPIE The International Society for Optical Engineering, vol. 1776, 1992, 226–234.
[67] B. Turton, T. Arslan, D. Horrocks, A hardware architecture for a parallel genetic algorithm for image registration, in: IEEE Colloquium on Genetic Algorithm in Image Processing and Vision, IEEE Computer Society, 1994, 111–116.
[68] G. Ou, H. Chen, W. Wang, Real-time image registration based on genetic algorithms, in: First International Conference on Real Time Imaging, IEEE Computer Society, 1996, 172–176.
[69] P. Chalermwat, T.A. El-Ghazawi, Multi-resolution image registration using genetics, in: International Conference on Image Processing, vol. 2, 1999, 452–456.
[70] T. Kim, Y. Im, Automatic satellite image registration by combination of stereo matching and random sample consensus, IEEE Trans. Geosci. Remote Sens. 41 (5) (2003) 1111–1117.
[71] Y.S. Oh, D.G. Sim, R.H. Park, R.C. Kim, S.U. Lee, I.C. Kim, Absolute position estimation using IRS satellite images, ISPRS J. Photogrammetry Remote Sens. 60 (4) (2006) 256–268.
[72] L. Tian, S.I. Kamata, Voting Weighted Modified Hausdorff Distance Through Multiscale Space for Automatic Image-Map Registration, in: Eighteenth International Conference on Pattern Recognition (ICPR'06), IEEE Computer Society, 2006, 837–840.
[73] F. Calderon, J.J. Flores, L. Romero, Robust parametric image registration, in: Hybrid Evolutionary Algorithms, Series: Studies in Computational Intelligence, vol. 75, Springer, (2007), p. 207.
[74] R. Storn, K. Price, Differential evolution - a simple and efficient heuristic for global optimization over continuous spaces, J. Global Optimization 11 (4) (1997) 341–359.
[75] K. Price, R. Storn, J. Lampinen, Differential Evolution: A Practical Approach to Global Optimization, Natural Computing Series, Springer-Verlag, 2005.
[76] M. Omran, A.P. Engelbrecht, A. Salman, Differential evolution methods for unsupervised image classification, in: IEEE Congress on Evolutionary Computation, vol. 2, IEEE Press, Piscataway NJ, (2005), pp. 966–973.
[77] I. De Falco, A. Della Cioppa, E. Tarantino, Automatic classification of handsegmented image parts using differential evolution, in: Lecture Notes in Computer Science, vol. 3907, Springer-Verlag, 2006, pp. 403–414.
[78] X. Dai, S. Khorram, A feature-based image registration algorithm using improved chain-code representation combined with invariant moments, IEEE Trans. Geosci. Remote Sens. 37 (5) (1999) 2351–2362.
[79] K. Rohr, Landmark-based Image Analysis: Using Geometry and Intensity Models, vol. 21 of Computational Imaging and Vision Series, Kluwer Academic Publisher, 2001.
[80] Y. Lim, M. Kim, T. Kim, S. Cho, Automatic precision correction of satellite images using the gcp chips of lower resolution, in: IEEE International Geoscience and Remote Sensing Symposium, vol. 2, Anchorage, Alaska, USA, (2004), pp. 1394–1397.
[81] P. Thomas, D. Vernon, Image registration by differential evolution, in: Irish Machine Vision and Image Processing Conference, Magee College, University of Ulster, Ireland, (1997), pp. 221–225.
[82] W. Wen-Hao, C. Yung-Chang, Image registration by control points pairing using the invariant properties of line segments, Pattern Recognit. Lett. 18 (3) (1997) 269–281.
[83] N.S. Netanyahu, J. Le Moigne, J.G. Masek, Georegistration of landsat data via robust matching of multiresolution features, IEEE Trans. Geosci. Remote Sens. 42 (2004) 1586–1600.
[84] F. Maes, A. Collignon, D. Vandermeulen, G. Marchal, P. Suetens, Multimodality image registration by maximization of mutual information, IEEE Trans. Med. Imaging 16 (2) (1997) 187–198.
[85] J.P.W. Pluim, A.J.B. Maintz, M.A. Viergever, Mutual-information-based registration of medical images: a survey, IEEE Trans. Med. Imaging 22 (2003) 986–1004.
[86] J.P.P. Starink, E. Baker, Finding point correspondence using simulated annealing, Pattern Recognit. 28 (1995) 231–240.
[87] P. Viola, W.M. Wells, Alignment by maximization of mutual information, Int. J. Comput. Vision 24 (1997) 137–154.
[88] H.S. Sawhney, R. Kumar, True multi-image alignment and its application to mosaicing and lens distorsion correction, IEEE Trans. Pattern Anal. Mach. Intell. 21 (1999) 235–243.
[89] M. Jenkinson, S. Smith, A global optimisation method for robust affine registration of brain images, Med. Image Anal. 5 (2001) 143–156.
[90] M. Salomon, G.R. Perrin, F. Heitz, Differential evolution for medical image registration, in: International Conference on Artificial Intelligence, Las Vegas, Nevada, USA, (2001), pp. 123–129.
[91] S. Winter, B. Brendel, C. Igel, Registration of bone structures in 3d ultrasound and ct data: Comparison of different optimization strategies, in: International Congress Series, vol. 1281, Elsevier Science, 2005, pp. 242–247.
[92] http://terraweb.wr.usgs.gov/projects/sfbay/.
[93] http://nayana.ece.ucsb.edu/registration/.
[94] D. Fedorov, L.M.G. Fonseca, C. Kenney, B.S. Manjunath, Automatic registration and mosaicking system for remotely sensed imagery, in: S.B. Serpico (Ed.), Proceedings of SPIE, vol. 4885, 2002, pp. 444–451.
[95] http://www.mathworks.com/.
[96] B.S. Manjunath, S.K. Le Mitra, A contour-based approach to multisensor image registration, IEEE Trans. Image Process. 4 (3) (1995) 320–334.
[97] http://www.aurigaimaging.com/.
[98] P. Tévenaz, U.E. Ruttimann, M. Unser, A pyramid approach to subpixel registration based on intensity, IEEE Trans. Image Process. 7 (1) (1998) 27–41.
[99] http://bigwww.epfl.ch/thevenaz/turboreg/.
[100] http://rsb.info.nih.gov/ij/.